

Photon cutting for excitation of Er^{3+} ions in SiO_2 sensitized by Si quantum dots

N. N. Ha,¹ S. Cueff,² K. Dohnalová,¹ M. T. Trinh,¹ C. Labbé,² R. Rizk,² I. N. Yassievich,³ and T. Gregorkiewicz¹

¹*Van der Waals-Zeeman Institute, University of Amsterdam, Science Park 904, NL-1098 XH Amsterdam, The Netherlands*

²*Centre de Recherche sur les Ions, les Matériaux et la Photonique (CIMAP), ENSICAEN, CNRS, CEA/IRAMIS, Université de Caen, F-14050 Caen Cedex, France*

³*A.F. Ioffe Physico-Technical Institute, Russian Academy of Sciences (RAS), 26 Polytekhnicheskaya, 194021 St. Petersburg, Russia*

(Received 16 November 2011; published 22 December 2011)

We present evidence of a mechanism for the indirect excitation of Er^{3+} ions in a SiO_2 matrix sensitized with Si quantum dots (SiQDs). The proposed process enables the simultaneous and rapid excitation of two proximal Er^{3+} ions upon absorption of a single high-energy photon in a SiQD. The experimental evidence leading to the identification of this energy-transfer path is obtained from investigations of the photoluminescence quantum yield of two Er-related emission bands at 1.54 and 0.98 μm in SiO_2 layers doped with small ($\sim 2\text{-nm}$ -diam) SiQDs and a high concentration of Er^{3+} ions, prepared by sputtering on hot substrates. In contrast to the previously considered mechanisms for the indirect excitation of Er^{3+} ions in SiO_2 , this excitation process offers an advantage of efficient suppression of the most important channels of nonradiative deexcitation—the Auger energy transfer to free carriers as well as the so-called energy back transfer of excitation reversal. This feature revives hopes for the practical application of Er-doped SiO_2 sensitized by SiQDs.

DOI: 10.1103/PhysRevB.84.241308

PACS number(s): 78.67.Bf, 78.60.Fi

Rare-earth (RE) ions are favorite “optical dopants” frequently used to tailor optical properties of insulating and semiconducting hosts. Following the success of neodymium-doped yttrium aluminum garnet (Nd:YAG), most attention has been given to Er-doped crystalline Si due to its emission wavelength coinciding with the absorption minimum of telecommunication networks. The research is motivated by prospective applications in Si photonics and optoelectronics.^{1,2} Unfortunately, while much information has been gathered and many interesting effects have been observed (e.g., Refs. 3 and 4), broader applications of Si:Er remain limited due to the thermal instability of emission. Among insulating hosts, the SiO_2 matrix doped with Er^{3+} ions ($\text{SiO}_2\text{:Er}$) is also well investigated as the basis for the development of optical amplifiers. However, due to the fact that the optical properties of RE ions are determined by the inner $4f$ electron shell, the $\text{SiO}_2\text{:Er}$ -based amplifiers require high-power resonant pumping, which is cumbersome and expensive.

Excitation of photo- and electro-luminescence of Er^{3+} ions in SiO_2 can be effectively sensitized by Si quantum dots (SiQDs).^{5–9} In this case, room-temperature 1.54- μm Er-related emission can be induced by a nonresonant excitation process via band-to-band absorption in SiQDs. Since the indirect band structure of Si is preserved also in its nanocrystalline form,¹⁰ electron-hole pairs generated in this way are characterized by a relatively long lifetime, enabling energy transfer to Er^{3+} ions located in the vicinity. Making use of the band-to-band absorption, this indirect excitation process is relatively efficient, with an (effective) excitation cross section of $\sigma \approx 10^{-17}\text{--}10^{-16}$ cm^2 . As a result, an increase of a factor $\sim 10^3$ in σ is found in comparison with $\text{SiO}_2\text{:Er}$,⁸ while at the same time it is $\sim 10^3$ times lower than for Si:Er.¹¹ It can be therefore concluded that the solid-state dispersion of SiQDs in an Er-doped SiO_2 matrix— $\text{SiO}_2\text{:Er,SiQDs}$ —to a certain extent combines positive features of Er-doped crystalline Si with the advantages of Er-doped SiO_2 : a high excitation cross section and temperature-stable emission. However, despite the

continuous developments in the preparation of the $\text{SiO}_2\text{:Er,SiQDs}$ material, only a relatively small proportion of all the Er^{3+} ions is usually available for indirect excitation via SiQDs.^{12,13} This limitation is the main obstacle in attaining a high concentration of excited Er^{3+} ions and population inversion, which is necessary for optical amplification.¹⁴ Obviously, this problem relates to the microscopic details of the indirect excitation mechanism. Dedicated experiments^{15,16} have revealed that the excitation of Er^{3+} ions in the $\text{SiO}_2\text{:Er,SiQDs}$ system involves mechanisms operating on different time scales, from several microseconds down to below 100 ns. In particular, the Förster (dipole-dipole) mechanism^{17,18} has been proposed in order to explain the “slow” (microsecond time scale) energy transfer from SiQDs, to Er^{3+} ions,¹⁹ and the microscopic location of Er with respect to SiQDs has been considered.^{20,21} In addition to this relatively slow excitation, the presence of a much faster (sub-100-ns range) process has been conclusively established.^{15,22} As for its physical origin, a process analogous to hot-carrier impact excitation of Er in bulk Si has been put forward.^{15,16} In this mechanism a hot carrier loses (part of) its excess energy by intraband relaxation with energy transfer to an Er^{3+} ion.

In this work, we present investigations of the optical excitation of Er^{3+} ions in the $\text{SiO}_2\text{:Er,SiQDs}$ material with a high Er concentration. We demonstrate evidence of a very specific energy-transfer path, in which two Er^{3+} ions are excited simultaneously by a single photon of sufficiently high energy absorbed in a SiQD. This excitation mechanism is enabled by the proximity of Er dopants and bears a strong similarity to quantum cutting observed for RE ions.²³ It operates parallel to the earlier reported Förster dipole-dipole process and Auger-facilitated energy-transfer mechanisms. The identification is based on the analysis of the quantum yield of two Er-related emission bands at 1.54 and 0.98 μm , appearing due to the radiative recombination from the first ($^4I_{13/2} \rightarrow ^4I_{15/2}$) and second ($^4I_{11/2} \rightarrow ^4I_{15/2}$) excited states of Er^{3+} ions, respectively.

The study has been performed on a series of $\text{SiO}_2:(\text{Er},\text{SiQDs})$ samples with a thickness of $1\text{--}2\ \mu\text{m}$ prepared by radio-frequency magnetron co-sputtering on hot ($500\ ^\circ\text{C}$) quartz substrates. A Si excess of $\sim 8.5\ \text{at.}\ \%$ and an Er concentration of $[\text{Er}] \approx 1\text{--}2 \times 10^{20}\ \text{cm}^{-3}$ were estimated via energy-dispersive x-ray spectroscopy. Subsequently, the samples were annealed at temperatures ranging from 600 to $1100\ ^\circ\text{C}$. The combination of the hot substrate growth and high-temperature annealing resulted in the elimination of defect centers and the formation of small Si nanoclusters of $\sim 2\ \text{nm}$ diameter. Further details of the sample preparation procedure and material characterization can be found elsewhere.^{24,25} Following preliminary selection, samples with the most intense $1.54\text{-}\mu\text{m}$ Er-related emission have been chosen for the investigation of optical properties.

The tunable excitation in the UV-vis range has been provided by a system of two coupled optical parametric oscillators pumped by the third harmonic of a Nd:YAG laser, delivering 5-ns pulses with a repetition rate of 10 and $100\ \text{Hz}$ (Solar Laser Systems). The photoluminescence (PL) signals were collected in a monochromator—either THR-1000, $f/8$, 900 grooves/mm (Jobin-Yvon) or $f/3.8$, 600 grooves/mm (Solar Laser Systems). The signals were detected by a nitrogen-cooled InGaAs photomultiplier tube (Hamamatsu R5509-72) or a germanium detector (Edinburgh Instruments) in combination with a lock-in amplifier (Signal Recovery SR7265) and/or a digital oscilloscope (Tektronix TDS3000). The analysis has been based on time-integrated PL signals. All experiments were carried out at room temperature.

In order to evaluate the quantum yield for a particular PL band, the PL intensity measured at different excitation wavelengths had been scaled to an equal number of absorbed photons. Therefore, the excitation power for a certain excitation photon energy E_{exc} was tuned using the following relation:

$$P(\lambda) = \Phi(\lambda)E_{\text{exc}} \propto \frac{E_{\text{exc}}}{1 - e^{-\text{OD}(\lambda)\ln 10}},$$

where $\Phi(\lambda)$ is the pumping photon flux, and $\text{OD}(\lambda)$ is optical density of the sample. The latter was determined from the Lambert-Beer absorption profile using a UV-Vis Lambda900 spectrometer in combination with an integrating sphere.

As mentioned above, the SiQD-assisted indirect excitation of Er^{3+} ions in SiO_2 is a multichannel process, with different mechanisms operating in parallel. For a particular material, with fixed SiQD size and distribution, and a certain concentration of Er^{3+} ions, the relative contributions of these excitation channels are expected to vary with the excitation photon energy. In the Förster energy-transfer process, the nonradiative recombination of an electron-hole pair in the core of a SiQD is accompanied by the excitation of an adjacent Er^{3+} ion via the dipole-dipole interaction. The energy mismatch is compensated by phonon emission, which reduces efficiency of the transfer. This process is relatively slow and critically dependent on the mutual separation between the SiQD and the Er^{3+} ion. In the present case, the maximum of the PL spectrum of SiQDs in the investigated material (see the inset to Fig. 1) is $\sim 1.8\ \text{eV}$. Therefore, in view of the energy conservation, the Förster energy transfer into the first $^4I_{13/2}$ is highly improbable, and will proceed through the second $^4I_{11/2}$, the third $^4I_{9/2}$ or even higher excited states of the Er^{3+} ion, depending on the

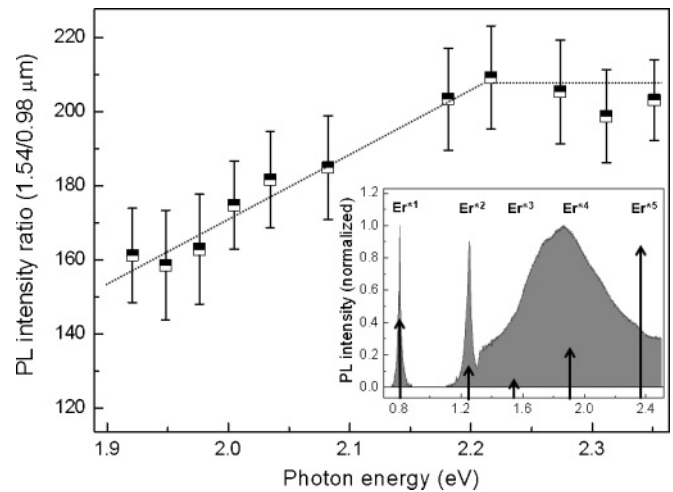


FIG. 1. The ratio between the PL intensities of the first ($1.54\ \mu\text{m}$) and the second ($0.98\ \mu\text{m}$) excited states of Er^{3+} ions in $\text{SiO}_2:(\text{Er},\text{SiQDs})$ as a function of excitation photon energy. The complete PL spectrum of the investigated sample is shown in the inset, with the indication of the energy levels of excited states of Er^{3+} ions in comparison with the photon emission energy. The Er^{*i} ($i = 1\text{--}5$) corresponds to the $^4I_{13/2}$ ($0.81\ \text{eV}$), $^4I_{11/2}$ ($1.26\ \text{eV}$), $^4I_{9/2}$ ($1.55\ \text{eV}$), $^4F_{9/2}$ ($1.9\ \text{eV}$), and $^2H_{11/2}$ ($2.38\ \text{eV}$) excited states of the Er^{3+} ions, respectively.

optical band gap of the involved SiQD. Thus, the $1.54\text{-}\mu\text{m}$ emission can only appear following the internal relaxation of the $4f$ -electron shell into the emitting $^4I_{13/2}$ state, which takes place on a microsecond time scale. Therefore, in the case that the Förster energy-transfer process would be the only available excitation path for Er^{3+} ions, the intensity ratio of emissions from the first (at $1.54\ \mu\text{m}$) and the second (at $0.98\ \mu\text{m}$) excited states should be independent on excitation photon energy, being solely governed by the internal relaxation of the inner $4f$ -electron shell. This is not observed in the experiment: The intensity ratio of the Er-related PL bands at 1.54 and $0.98\ \mu\text{m}$ as measured under excitation with different photon energies E_{exc} is presented in the main panel of Fig. 1. As can be seen, the relative intensity of the $1.54\text{-}\mu\text{m}$ band rises with higher excitation energy, until $E_{\text{exc}} \approx 2.1\ \text{eV}$. We conclude that in our material the Förster energy transfer is not the only excitation mechanism and must be accompanied by another process transferring energy directly into the $^4I_{13/2}$ state. This situation changes for even higher excitation photon energies $E_{\text{exc}} \gtrsim 2.1\ \text{eV}$, as the intensity ratio of the two bands becomes constant.

The increased emission at $1.54\ \mu\text{m}$ could be induced by the aforementioned Auger process of impact excitation by hot carriers. According to previous investigations,^{15,16} the impact excitation process requires a minimum excess energy of the excited carrier of $0.81\ \text{eV}$, necessary to bring an Er^{3+} ion into the $^4I_{13/2}$ state. In that case, the minimum excitation photon energy marking the onset of the impact excitation should be $E_{\text{exc}}^{\text{imp}} = E_g + 0.81\ \text{eV}$, where $E_g \approx 1.8\ \text{eV}$ is the “optical band gap” of SiQDs facilitating the process. Such a threshold value indeed has been confirmed in the past for a $\text{SiO}_2:(\text{Er},\text{SiQDs})$ material with a lower Er concentration of $[\text{Er}] \approx 2.8 \times 10^{19}\ \text{cm}^{-3}$.²⁶ In the present case, $E_g \approx 1.8\ \text{eV}$,

as determined from the excitonic emission of the investigated sample in the inset to Fig. 1, leading to $E_{\text{exc}}^{\text{imp}} \approx 2.6$ eV. From Fig. 1, we see that the PL intensity ratio changes already for excitation photon energies that are much below this estimated value, with the increase practically commencing just above the optical band gap E_g . We conclude that the previously proposed impact excitation mechanism cannot account for the current results, and that a different explanation has to be sought.

Looking for a possible excitation process which could account for the experimental findings, we recall that in the past also an excitation mechanism involving participation of a not well specified type of defect center has been proposed for Er in Si-rich SiO_2 .²⁷ However, in the present case the formation of defects in the investigated materials has been purposefully suppressed by the use of hot substrates and post-growth high-temperature annealing. Therefore, the presence of a sufficiently large number of defect centers to facilitate an efficient excitation route is unlikely.

In order to gain further insight into the possible microscopic mechanism responsible for the experimental observations, we have investigated the (external) quantum yield (QY) of both Er-related PL bands, in the energy range where their intensity ratio varied, below the estimated threshold for impact excitation. The results are depicted in Fig. 2. The experiments were conducted under the condition of an equal number of absorbed photons and in the low excitation flux regime to exclude nonlinear effects. For a simple comparison, the QY values obtained for both bands have been normalized for the lowest excitation energy. (In fact, the QY of the 1.54- μm band was found to be two orders of magnitude higher than that of the 0.98- μm emission.) We see that the QY of the 1.54- μm band increases practically over the whole range of the investigated excitation energies. In contrast, the QY of the 0.98- μm band remains constant for lower excitation photon energy and increases only above the threshold value of ~ 2.1 eV. We point out that the QY data depicted in Fig. 2 are fully consistent with the PL intensity ratio given in Fig. 1, and show

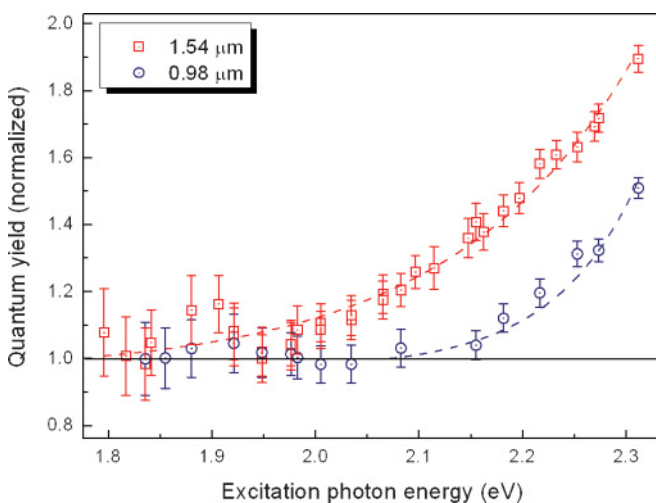


FIG. 2. (Color online) The dependence of quantum yield (QY) of both emission bands at 0.98 μm (blue circles) and 1.54 μm (red squares) on the excitation photon energy under the condition of an equal number of absorbed photons per pulse ($9 \times 10^{10} \text{ cm}^{-2}$), in the low excitation regime.

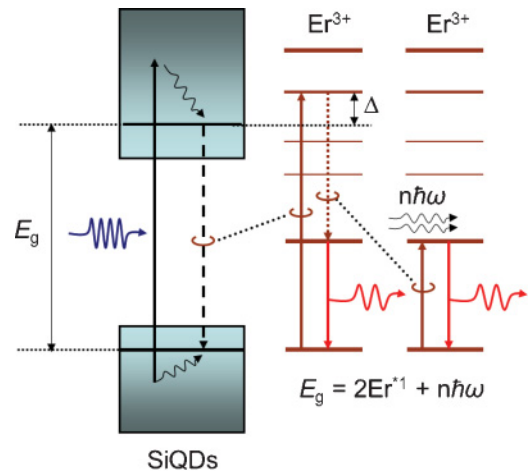


FIG. 3. (Color online) Schematic illustration of the nonresonant excitation mechanism, via the high excited state of Er as the virtual state (second-order perturbation process), leading to the simultaneous excitation of two neighboring Er ions in the first excited state (Er^{*1}) under absorption of a single photon. Δ is the energy mismatch between the exciton ground state and the virtual state involved.

that additional excitation below the estimated threshold for impact excitation process takes place not only into the lower $^4I_{13/2}$ but also into the higher $^4I_{11/2}$ state of the Er^{3+} ions.

Before proposing a different physical mechanism, we note that a high-energy carrier can be generated also by sequential absorption of two low-energy photons; it is possible that a photo-generated carrier might absorb another photon (intra-band absorption), and attain a higher excited state, enabling the impact excitation mechanism. As a result, the threshold for this process might be shifted to a lower excitation photon energy. In order to exclude this possibility, we investigated the QY of the 1.54- μm band for all photon energies under low and high flux conditions. Both dependencies were linear and practically identical in the measured energy range, directly scaling with the flux ratio ($55\times$). We conclude that the generation of hot carriers due to intraband absorption can be neglected. Therefore, the increase of the QY observed for excitation energies below the impact excitation threshold indicates the presence of a different excitation mechanism.

The proposed energy-transfer process which can account for the experimental findings reported in this study is schematically depicted in Fig. 3. In the first step a photon of energy larger than the band gap is absorbed by a SiQD generating an exciton, possibly with some excess energy. The excitation process proceeds by a Coulombic interaction of an exciton in the ground state and the nearest Er^{3+} ion.²⁸ In this case, one of higher excited states of the Er^{3+} ion acts as a virtual state enabling the process—the i th excited state in the inset to Fig. 1. It is the second-order perturbation process, in which the next step involves an immediate transfer of part of the energy to the second Er^{3+} ion in close proximity, enabled in our material by the high concentration of Er dopants. Thus the final state of the process comprises two Er^{3+} ions in excited states, while the possible energy excess is compensated by (multi)phonon emission. The efficiency of the proposed process is higher for a smaller energy mismatch Δ between the exciton and the

virtual state (see Fig. 3) and depends also on the oscillator strength of the involved excited state of Er^{3+} . In contrast to the impact excitation, in the present case no free carriers are left after excitation is completed, thereby limiting deexcitation by the Auger process. At the same time, the fact that Er^{3+} ions are excited into the lower excited states while the band-gap energy of the SiQDs is relatively large limits the excitation reversal by the so-called back-transfer process,²⁹ in which the energy disperses back to SiQDs. The probability of the excitation process via a virtual state can compete with excitation into the real Er^{3+} state of lower energy, as it involves the higher states of the Er^{3+} ions with higher oscillator strengths and is assisted by lower numbers of the emitted phonons, and increases dramatically with Er concentration. The complete theoretical model of the proposed mechanism and a detailed evaluation of the transition probabilities will be presented in a separate publication.

The process depicted in Fig. 3 provides an additional efficient Er excitation channel that can account for the QY enhancement. Excitons in the ground state of SiQDs with band-gap energies above 1.62 eV can excite two Er^{3+} ions into the first excited state ($E_g > 2 \times 0.81$ eV), upon a single photon absorption, explaining the rise of its QY in Fig. 2. The excitons in SiQDs with a band-gap energy larger than the sum of the first and the second excited states of the Er^{3+} ions ($E_g > 0.81 + 1.24$ eV = 2.05 eV) can facilitate the excitation process in which one Er^{3+} ion attains the first excited state $^4I_{13/2}$, giving rise to the 1.54- μm emission, while the second one goes to the second excited state $^4I_{11/2}$, enhancing the 0.98- μm PL, stabilizing the ratio of 1.54- and 0.98- μm emissions shown for higher energies (Fig. 1).

In conclusion, the current study shows that the indirect excitation of Er^{3+} ions in SiO_2 facilitated by SiQDs is a complex multi-channel process with the participation of different physical mechanisms. Their individual contributions depend on the pumping photon energy but also on material characteristics. In particular, for the $\text{SiO}_2:(\text{Er},\text{SiQDs})$ system with small SiQDs and a sufficiently large Er concentration, we identify a unique energy-transfer mechanism in which two Er^{3+} ions can be simultaneously excited upon absorption of a single photon of sufficiently high energy. The process involves direct photon energy transfer into two Er^{3+} ions, assisted by a SiQD. In comparison with previously identified excitation mechanisms taking place in the $\text{SiO}_2:(\text{Er},\text{SiQDs})$ system—the impact excitation and energy transfer by the dipole-dipole interaction (Förster)—the proposed mechanism offers the important advantage of suppressing the most important processes of non-radiative de-excitation that hamper the practical potential of this material for applications—the Auger process of energy transfer to free carriers and excitation reversal by back-transfer. Finally, we note that the proposed mechanism bears some similarity with the previously reported quantum cutting taking place between two types of different rare-earth ions or the Er^{3+} ions themselves,³⁰ while removing the disadvantage of resonant pumping, thanks to the band-to-band absorption in SiQDs.

The authors wish to thank O. B. Gusev for useful discussions. This work is part of the research program of the Stichting voor Fundamenteel Onderzoek der Materie (FOM), financially supported by De Nederlandse Organisatie voor Wetenschappelijk Onderzoek (NWO).

-
- ¹A. J. Kenyon, *Semicond. Sci. Technol.* **20**, R65 (2005).
²N. Q. Vinh, N. N. Ha, and T. Gregorkiewicz, *Proc. IEEE* **97**, 1269 (2009).
³M. Forcales, T. Gregorkiewicz, I. V. Bradley, and J. P. R. Wells, *Phys. Rev. B* **65**, 195208 (2002).
⁴N. Q. Vinh, H. Przybylińska, Z. F. Krasil'nik, and T. Gregorkiewicz, *Phys. Rev. B* **70**, 115332 (2004).
⁵A. J. Kenyon, P. F. Trwoga, M. Federighi, and C. W. Pitt, *J. Phys. Condens. Matter* **6**, L319 (1994).
⁶M. Fujii, M. Yoshida, Y. Kanzawa, S. Hayashi, and K. Yamamoto, *Appl. Phys. Lett.* **71**, 1198 (1997).
⁷C. E. Chryssou, A. J. Kenyon, T. S. Iwayama, C. W. Pitt, and D. E. Hole, *Appl. Phys. Lett.* **75**, 2011 (1999).
⁸D. Pacifici, G. Franzò, F. Priolo, F. Iacona, and L. Dal Negro, *Phys. Rev. B* **67**, 245301 (2003).
⁹P. G. Kik, M. L. Brongersma, and A. Polman, *Appl. Phys. Lett.* **76**, 2325 (2000).
¹⁰D. Kovalev, H. Heckler, M. Ben-Chorin, G. Polisski, M. Schwartzkopff, and F. Koch, *Phys. Rev. Lett.* **81**, 2803 (1998).
¹¹O. B. Gusev, M. S. Bresler, P. E. Pak, I. N. Yassievich, M. Forcales, N. Q. Vinh, and T. Gregorkiewicz, *Phys. Rev. B* **64**, 075302 (2001).
¹²M. Wojdak, M. Klik, M. Forcales, O. B. Gusev, T. Gregorkiewicz, D. Pacifici, G. Franzò, F. Priolo, and F. Iacona, *Phys. Rev. B* **69**, 233315 (2004).
¹³P. G. Kik and A. Polman, *J. Appl. Phys.* **88**, 1992 (2000).
¹⁴N. N. Ha, K. Dohnalová, T. Gregorkiewicz, and J. Valenta, *Phys. Rev. B* **81**, 195206 (2010).
¹⁵I. Izeddin, A. S. Moskalenko, I. N. Yassievich, M. Fujii, and T. Gregorkiewicz, *Phys. Rev. Lett.* **97**, 207401 (2006).
¹⁶I. Izeddin, D. Timmerman, T. Gregorkiewicz, A. S. Moskalenko, A. A. Prokofiev, I. N. Yassievich, and M. Fujii, *Phys. Rev. B* **78**, 035327 (2008).
¹⁷T. Förster, *Ann. Phys.* **2**, 55 (1948).
¹⁸V. M. Agranovich and M. D. Galanin, *Electronic Excitation Energy Transfer in Condensed Matter* (Elsevier, Amsterdam, 1982).
¹⁹M. J. A. de Dood, J. Knoester, A. Tip, and A. Polman, *Phys. Rev. B* **71**, 115102 (2005).
²⁰X. L. Wu, Y. F. Mei, G. G. Siu, K. L. Wong, K. Moulding, M. J. Stokes, C. L. Fu, and X. M. Bao, *Phys. Rev. Lett.* **86**, 3000 (2001).
²¹R. A. Senter, C. Pantea, Y. Wang, H. Liu, T. W. Zerda, and J. L. Coffey, *Phys. Rev. Lett.* **93**, 175502 (2004).
²²M. Fujii, K. Imakita, K. Watanabe, and S. Hayashi, *J. Appl. Phys.* **95**, 272 (2004).
²³R. T. Wegh, H. Donker, K. D. Oskam, and A. Meijerink, *Science* **283**, 663 (1999).
²⁴S. Cuff, C. Labbé, B. Dierre, F. Fabbri, T. Sekiguchi, X. Portier, and R. Ritzk, *J. Appl. Phys.* **108**, 113504 (2010).

- ²⁵S. Cueff, C. Labbé, B. Dierre, J. Cardin, L. Khomenkova, F. Fabbri, T. Sekiguchi, and R. Rizk, *J. Nanophotonics* **5**, 151504 (2011).
- ²⁶D. Timmerman, I. Izeddin, P. Stallinga, I. N. Yassievich, and T. Gregorkiewicz, *Nat. Photon.* **2**, 105 (2008).
- ²⁷O. Savchyn, F. R. Ruhge, P. G. Kik, R. M. Todi, K. R. Coffey, H. Nukala, and H. Heinrich, *Phys. Rev. B* **76**, 195419 (2007).
- ²⁸I. N. Yassievich, *Opt. Mater.* **33**, 1079 (2011).
- ²⁹A. A. Prokofiev, I. N. Yassievich, H. Vrielinck, and T. Gregorkiewicz, *Phys. Rev. B* **72**, 045214 (2005).
- ³⁰M. Miritello, R. Savio, P. Cardile, and F. Priolo, *Phys. Rev. B* **81**, 041411 (2010).